UDK 621.9.048
Original scientific article/Izvirni znanstveni članek

ISSN 1580-2949
MTAEC9, 56(2)131(2022)

EXPERIMENTAL INVESTIGATION OF ELECTRICAL DISCHARGE MACHINING OF INCONEL 718 USING A TiB_2-Cu SINTERED COMPOSITE ELECTRODE

EKSPERIMENTALNE RAZISKAVE EROZIJSKE OBDELAVE SUPERZLITINE INCONEL 718 Z UPORABO SINTRANE KOMPOZITNE ELEKTRODE TiB_2-Cu

P. Mathan Kumar*, K. Sivakumar, Vinu Kumar S. M.

Department of Mechanical Engineering, Bannari Amman Institute of Technology, Sathyamangalam 638401, India

Prejem rokopisa – received: 2022-01-12; sprejem za objavo – accepted for publication: 2022-01-31

doi:10.17222/mit.2022.368

Electrical discharge machining (EDM) is much preferred in modern precision-manufacturing industries owing to its ability to machine any metal regardless of its hardness. However, its constraint is that the selected metal should be an electrically conductive material. For the present investigation, an Inconel 718 alloy was selected for EDM, using a TiB_2-Cu electrode made with powder metallurgy. Input factors, namely, the pulse current (I_p), pulse-on time (T_{on}) and gap voltage (G_v) were selected and their output responses were the surface roughness (SR) and material-removal rate (MRR). For the response surface, the Box Behnken technique was preferred when designing the experiments (DoE). An ANOVA test was performed to understand the influence of the selected input factors on the SR and MRR. The RSM integrated with a grey relational analysis (GRA) revealed that the optimal input parameters for better machining characteristics were: I_p = 10 A, T_{on} = 40 µs and G_v = 50 V. Besides, the results also showed that the pulse current more significantly influenced the output responses than the other parameters. Moreover, an increase in the gap voltage caused surface irregularities on the machined surface. Surface morphology of the machined surfaces was analysed through SEM and EDAX. Moreover, a certain amount of tool-material transfer was noted with the EDAX analysis.

Keywords: electrical discharge machining, powder metallurgy, Inconel 718, response surface methodology

Obdelava z erozijo oziroma električnim razelektrenjem v obloku (EDM; angl.: electric discharge machining) je postopek mehanske obdelave, ki se danes zelo uporablja v modernih industrijah različnih izdelkov zelo točnih dimenzij in toleranc, zaradi njegove sposobnosti obdelave katerega koli kovinskega materiala, ne glede na njegovo trdoto in ostale lastnosti. Vendar pa je omejitev tega postopka ta, da mora biti kovinski obdelovanec iz električno prevodnega materiala. V raziskavi, ki je opisana v članku, je bila za obdelavo z EDM izbrana Ni superzlitina Inconel 718 in uporabljena sintrana TiB_2-Cu elektroda. Izbrani vhodni procesni parametri so bili: pulzni električni tok (I_p), čas tokovnega impulza (T_{on}) in napetost v reži med obdelovancem in elektrodo (G_v). Izbrana opazovana parametra procesa EDM pa sta bila: hrapavost površine obdelovanca (SR) in hitrost odvzema materiala (MRR). Za načrtovanje in optimizacijo eksperimentov oziroma stanja površine po obdelavi z EDM pa je bila uporabljena tako imenovana Box-Behnkenovo tehnika. Izvedena je bila analiza variance ANOVA (angl.: analysis of variance) za razumevanje vpliva izbranih vhodnih parametrov na SR in MRR. Zabrisana relacijska analiza (GRA; angl.: grey relational analysis) integrirana v metodologijo odgovora površine (RSM; angl.: response surface methodology) je podala optimalne vhodne parametre EDM obdelave, in sicer: I_p = 10 A, T_{on} = 40 µs in G_v = 50 V. Rezultati analiz so pokazali, da ima pulzirajoči električni tok večji vpliv na hrapavost površine in odvzem materiala kot druga dva parametra. Poleg tega pa je povečanje napetosti v reži med obdelovancem in elektrodo povzročilo površinske nepravilnosti na obdelovancu. Morfologija obdelane površine je bila analizirana s pomočjo vrstičnega elektronskega mikroskopa (SEM) in rentgenske energijske disperzijske spektroskopije (EDAX). Slednja je pokazala določeno količino prenosa materiala z elektrode in dielektrika (olje) na površino obdelovanca.

Ključne besede: mehanska obdelava z erozijo, metalurgija prahov, Inconel 718, metodologija odgovora površine

1 INTRODUCTION

The EDM process is the most accepted and widely practiced manufacturing process in the field of die-making industries. It is an electro-thermal energy-based process where workpieces are machined mainly due to melting and vaporization.[1] In this process, direct contact between the workpiece and electrode is completely eliminated. With the conventional technique, it was challenging to produce complex-shaped tools made of materials (W, WC, ZrB_2, Ti) with a higher hardness. However, by employing powder metallurgy (PM), it is feasible to make any complex shape with the desired properties. The frequent flaws observed in EDM are a low MRR and high tool-wear rate. To overcome these shortcomings, electrodes made with powder metallurgy were employed and they have been successfully used according to different researchers.[1,2] Further, this process is cost-effective and does not require any additional set-up.[2] Gill et al.[3] machined the En31 tool steel using a Cu-W PM composite electrode to analyse the microhardness after EDM. The results revealed that the microhardness of the tool was enhanced. Teng et al.[4] studied the machining characteristics of a polycrystalline diamond using an Cu-Ni PM electrode in EDM. The study reported a rise in the MRR and decrease in the TWR. Sarmah et al.[5] prepared a powder-metallurgy Inconel aluminium tool for EDM to machine an Al-7075 alloy. The investigation clearly indi-

*Corresponding author's e-mail:
mathan129@gmail.com

cated an improvement in the microhardness of the machined surface. Kumar et al.[6] fabricated a Cu-TiB_2 PM electrode for EDM to study the MRR and tool-wear rate on the Monel 400TM alloy. An improvement in the MRR and reduction in the tool-wear rate were reported. Tanjilul et al.[7] selected a super-dielectric medium to drill into a nickel-based Inconel alloy in EDM. They concluded that the super-dielectric medium was capable of performing in an efficient manner in EDM. Jafarian[8] optimized the input factors in EDM involving Inconel 718 using the ANN technique. The hybrid ANN and NSGA were found to be suitable for analysing the performance of EDM.

Paswan et al.[9] machined Inconel 718, considering selected parameters of EDM and using a graphene nanofluid. An improvement in the surface morphology was noticed through FE-SEM images. Ramuvel et al.[10] investigated the effect of the input factors on the MRR and tool-wear rate using RSM as the design tool. They developed a quadratic model to predict the performance of the selected input factors in EDM for tool steel. Kumar et al.[11] derived the optimal setting for EDM input process parameters, using the Taguchi-GRA technique. Mazarbhuiya et al.[12] fabricated a copper-tungsten green compact PM electrode to create a complex profile of an aluminium 6061 workpiece. The ratio of tungsten and copper was about 25 *w*/% Cu to 75 *w*/% W. An improvement in the microhardness was observed when using the PM electrode. Li et al.[13] made an attempt to machine the GH2132 superalloy with EDM. To perform the experiments, Taguchi DoE was employed. The performance was evaluated by choosing the MRR, TWR and SR as the response parameters. Finally, the optimum parameter setting was identified with a GRA. Nair et al.[14] studied the machinability of Ti6Al4V work material in EDM using a brass electrode. They analysed the effect of the selected electrical input parameter on the surface integrity and microcracks. Their report suggested that the pulse discharge current had a crucial effect on the surface integrity and microcracks. Rahang et al.[15] fabricated a copper tungsten PM electrode to apply a coat on the selected surface of the workpiece. The electrode was not sintered in the furnace and it was in green form. The result showed that a certain amount of the tool material was exported to the machined surface and thus the hardness of the workpiece was enhanced.

Siddique et al.[16] prepared a PM electrode by mixing a copper-tungsten disulphide powder at different weight percentages. The objective for the developed electrode was to apply a coat layer to improve the surface property. The performance was analysed by observing the material-deposition rate and microhardness as the responses. Kumar et al.[17] performed an investigation on the behaviour of a CrB_2-Cu PM electrode on OHNS steel. Several electrodes were made, consisting of the proposed powders at different weight percentages. The selected electrode allowed better performance during the machining. The surface properties of the workpiece were analysed using a surface-roughness tester. An improvement in the wear resistance of the selected surface was reported. Chen et al.[18] attempted to drill a deep hole in an Inconel 718 alloy using EDM. The experiment was performed by adopting the RSM approach. The purpose of the study was to minimize the overcut effect in EDM and get the optimum setting for the desired outcome. Obratanski et al.[19] chose a titanium alloy for EDM using a graphite electrode. The study was performed under high current and T_{on}. Surface properties were evaluated through SEM and XRD analysis. Kumar et al.[20] chose an Inconel 825 alloy for EDM. The Al_2O_3 nanopowder mixed dielectric medium was chosen for machining and the changes in the machined surface were examined. The new dielectric material caused an increase in the material-removal rate compared to the conventional dielectric.

Mandal et al.[21] tested a new composite tool in EDM, which consisted of copper and carbon nanotubes. The test was conducted on a mild-steel workpiece. The effect of the composite electrode on the surface roughness was analysed. The formation of microcracks on the surface was considerably reduced due to the new electrode. Tyagi et al.[22] focused on the EDM of mild steel with a Cu-hBN green composite electrode. Composite pellets were fabricated at different weight percentages. The tribological properties of the machined surface were analysed. It was found that the wear resistance of the surface improved with the electrode. Sajeevam et al.[23] fabricated an Al-TiB_2 metal-matrix composite workpiece to be machined with EDM. The experiment was conducted in a chromium-powder mixed dielectric environment. The MRR and overcut were analysed using selected control variables. The selected composite was successfully tested with EDM. From the literature survey, it is evident that there has been a significant need for powder-metallurgy composite electrodes to enhance the material-removal rate and surface quality of EDM-machined workpieces that are mostly sought in the precision-manufacturing industries. Besides, it is also noted that only few studies have been reported in this domain. Henceforth, the present study was focused on fabricating a TiB_2-Cu composite electrode via powder metallurgy and analysing its performance in the machining of an Inconel 718 workpiece in EDM, using a multi-response optimization tool (GRA) integrated with the response-surface methodology.

2 EXPERIMENTAL PART

In this study, the TiB_2-Cu composite tool, prepared with powder metallurgy, was used as the electrode. A working schematic of the TiB_2-Cu powder-metallurgy electrode used in EDM is shown in **Figure 1**. Initially, the Cu powder and TiB_2 powder, each of 40 μm, were properly mixed in a V-blender for at least 2 h. This mixed powder was transported to a die for compaction where a uniform pressure of 10 MPa was applied to the die to get the desired pellet (5 mm). Subsequently, the

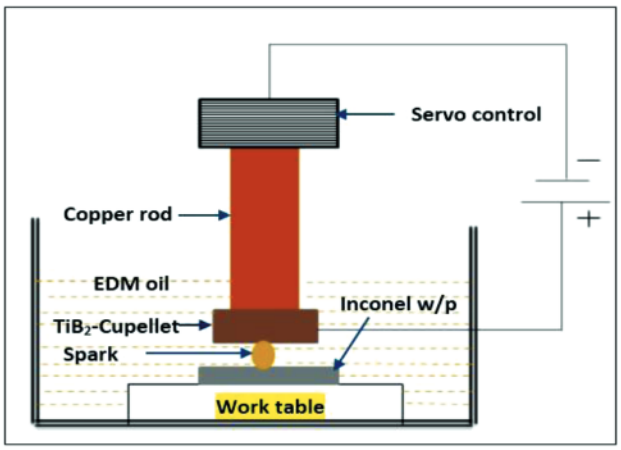

Figure 1: Schematic of the powder-metallurgy tool in EDM

pellet was brought to a tubular furnace to be sintered. The sintered pellet was then brazed with a conventional copper tool for machining. The final TiB_2-Cu composite pellet and the brazed electrode are shown in **Figure 2.** Inconel 718, a nickel-based alloy, was chosen to be machined in this study. This nickel alloy is widely used in jet-engine parts and high-speed airframe parts. For machining, a workpiece of (150 × 15 × 5) mm was selected and mounted on a vice.

Experiments were designed by employing the response-surface methodology (RSM). It is a statistical method, effectively utilized for planning experiments.[13] There are a few RSM methods used for designing experiments. In this study, the Box-Behnken approach was selected for designing the experiments. This approach mainly deals with the correlation between the input factors and output responses.[14] The optimum results can be obtained with a set of designed experiments. A second-degree polynomial model was formulated from the experimental results.

The Electra 5535 EDM set-up was used to machine Inconel 718. The Electra 5535 machine and the electrode setting are shown in **Figure 3**. An EDM dielectric oil was used as the medium for the experimentation. The experiments were conducted at positive polarity. The pulse-on time, pulse current and gap voltage were chosen as the input factors. The input factors and their level settings are shown in **Table 1**. The complete set of experiments was conducted based on the DoE shown in **Table 2**. The flushing pressure was kept at a constant level of 98.0665 kPa. The objective of the flushing was to remove the debris, formed during the machining process. Before starting the experimental work, it was important to conduct preliminary-experiment runs to find the working range of input control variables of the selected machine. The parameters were chosen based on the test runs and literature studies. The SR and MRR were chosen as the output responses. The MRR was determined using the formula shown as Equation (1). In order to weigh the workpiece before (W_b) and after the machining (W_a), a high-precision weighing machine was used. The machining time (T) was properly recorded to calculate the MRR. The SR was assessed using a surface-roughness tester. The EDM-machined Inconel 718 workpiece is shown in **Figure 4.**

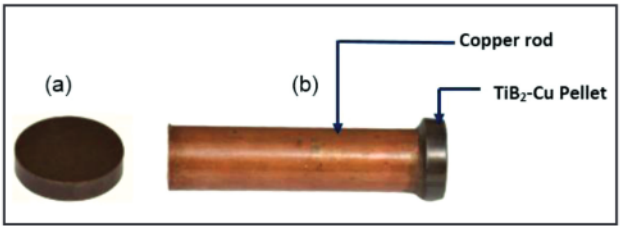

Figure 2: a) TiB_2-Cu pellet and b) working TiB_2-Cu electrode

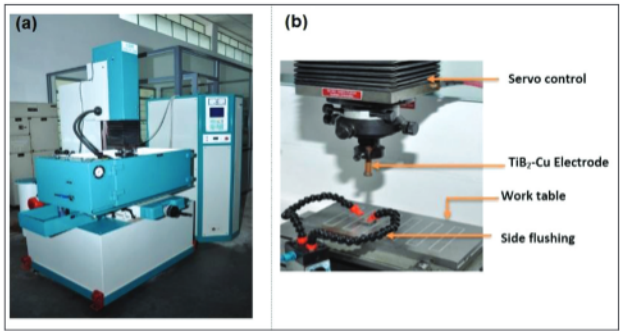

Figure 3: a) Electra 3355 EDM machine, b) EDM set-up

Figure 4: Samples of the machined workpiece

$$\mathrm{MRR} = \frac{W_b - W_a}{T} \quad (1)$$

Here, W_b and W_a indicate the weight of the workpiece before and after the machining (g), respectively. T indicates the time taken for the machining (min).

Table 1: EDM input process parameters and their levels

Variables	Units	Factors	Levels		
			−1	0	1
Pulse current	I_p/A	A	5	10	15
Pulse-on time	T_{on}/μs	B	40	80	120
Gap voltage	G_v/V	C	50	60	70

3 RESULTS AND DISCUSSION

The results for the MRR and SR obtained from the series of experiments are reported in **Table 2**. The second-order regression model for the MRR and SR was derived from these results. Equations (2) and (3) represent the regression models for the MRR and SR, respectively. An ANOVA test was performed to understand the influence of the selected input factor on the MRR and SR. The ANOVA results for the MRR and SR are shown in **Tables 3** and **4**, respectively. From the tables, it is clear

Table 2: Experimental design and determined MRR and SR

Run	I_p/A	T_{on}/μs	G_v/V	MRR/ (g/min)	SR/ μm
1	10	120	50	0.041	2.97
2	10	80	60	0.05	3.77
3	10	40	50	0.045	2.97
4	5	40	60	0.025	2.71
5	15	120	60	0.052	4.77
6	15	80	50	0.057	4.03
7	10	80	60	0.046	3.58
8	5	80	50	0.026	2.73
9	15	40	60	0.058	4.42
10	10	80	60	0.049	3.77
11	15	80	70	0.056	4.51
12	5	120	60	0.019	2.94
13	10	40	70	0.04	3.25
14	5	80	70	0.018	2.72
15	10	120	70	0.04	3.93

that the pulse current had the highest influence on the MRR and SR, followed by the pulse-on time and gap voltage. The obtained R^2 and adjusted R^2 values for the MRR are 98.26 % and 95.94 %, respectively, while for the SR, the values of R^2 and adjusted R^2 are 98.17 % and 94.97 %, respectively. From the ANOVA results, it is found that the developed model is significant and the lack of fit is insignificant.

The MRR has drawn attention from industries because it directly affects the production rate. Therefore, it is mandatory to analyse the impact of input/control factors on the MRR. **Figure 5a** illustrates the effects of the pulse current and pulse-on time with respect to the MRR. From **Figure 5a**, it is clear that I_p has a larger impact on the MRR than T_{on}. When the pulse current is 5 A, the MRR is found to be low, which may be attributed to the minimum energy dissipated from the electrode. Furthermore, a sudden increase in the MRR is observed as the pulse current increases from 5 A to 15 A, owing to the increase in the energy dissipation in the spark zone that led to a higher amount of the electrode heat energy.[7] Thus, large-size craters were found on the workpiece. On the other hand, the MRR increases gradually with respect to the pulse-on time ranging between 40 μs to 120 μs which may be because the pulse-on time produces an intense heating effect at the spark zone for a longer duration[17] and so the MRR increases. In **Figure 5b**, the relation between the pulse current and voltage, and its effect on the MRR are observed. It is found that a rise in the voltage led to a rise in the MRR which is attributed to the rise in the spark energy with respect to the voltage at the spark zone.[8] In comparison with the pulse current, voltage has a minimum influence on the MRR.

$$\text{MRR} = -0.086000 + (6.10833\times10^{-3}\ I_p) + (1.7916\times10^{-4}\ T_{on}) + (2.9125\times10^{-3}\ G_V) + (3.5\times10^{-5}\ I_pG_v) + (2.5\times10^{-6}\ T_{on}G_v) - (2.4166\times10^{-4}\ I_p^2) - (2.369\times10^{-6}\ T_{on}^2) - (3.0416\times10^{-5}\ G_V^2) \quad (2)$$

Table 3: ANOVA test results for the MRR

Source	Sum of squares	df	Mean square	F-value	P-value	
model	2.55×10^{-3}	9	2.83×10^{-4}	74.91	< 0.0001	significant
I_p	2.28×10^{-3}	1	2.28×10^{-3}	602.15	< 0.0001	
T_{on}	3.20×10^{-5}	1	3.20×10^{-5}	8.46	0.0335	
G_v	2.81×10^{-5}	1	2.81×10^{-5}	7.43	0.0415	
$I_p \times G_v$	1.23×10^{-5}	1	1.23×10^{-5}	3.24	0.1319	
$T_{on} \times G_v$	4.00×10^{-6}	1	4.00×10^{-6}	1.06	0.351	
I_p^2	1.35×10^{-4}	1	1.35×10^{-5}	35.62	0.0019	
T_{on}^2	5.31×10^{-5}	1	5.31×10^{-5}	14.03	0.0134	
G_v^2	3.42×10^{-5}	1	3.42×10^{-5}	9.03	0.0299	
residual	1.89×10^{-5}	5	3.78×10^{-6}	–	–	
lack of fit	1.03×10^{-5}	3	3.42×10^{-6}	0.79	0.6011	not significant
pure error	8.67×10^{-6}	2	4.33×10^{-6}	–	–	
cor total	2.57×10^{-3}	14	–	–	–	

Table 4: ANOVA test results for the SR

Source	Sum of squares	df	Mean square	F-value	P-value	
model	6.73	9	0.75	29.78	0.0008	significant
I_p	5.51	1	5.51	219.45	< 0.0001	
T_{on}	0.2	1	0.2	7.9	0.0375	
G_v	0.36	1	0.36	14.38	0.0127	
$I_p \times T_{on}$	3.60×10^{-3}	1	3.60×10^{-3}	0.14	0.7205	
$I_p \times G_v$	0.063	1	0.063	2.49	0.1755	
$T_{on} \times G_v$	0.12	1	0.12	4.6	0.0847	
I_p^2	0.044	1	0.044	1.75	0.2429	
T_{on}^2	0.041	1	0.041	1.65	0.2557	
G_v^2	0.38	1	0.38	15.13	0.0115	
residual	0.13	5	0.025	–	–	
lack of fit	0.1	3	0.034	2.81	0.2732	not significant
pure error	0.024	2	0.012	–	–	
cor total	6.86	14	–	–	–	

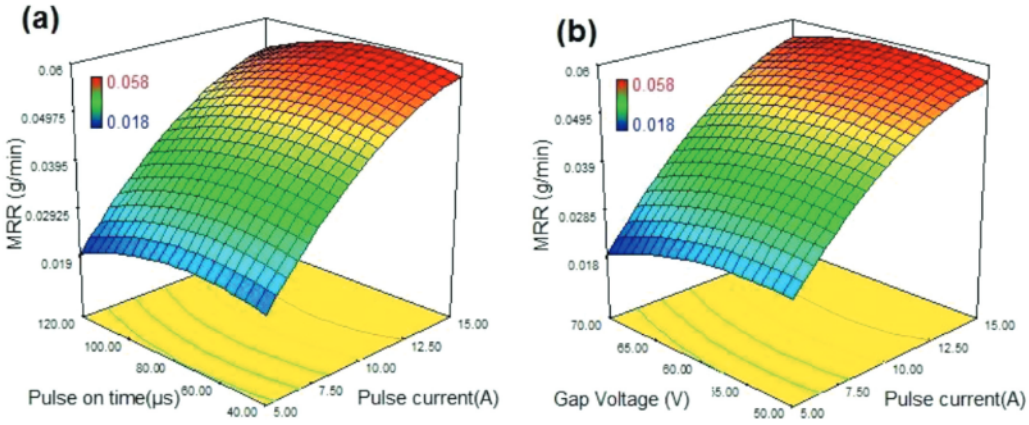

Figure 5: Effect on the MRR: a) I_p and T_{on}, b) I_p and G_v

The surface roughness is also a crucial response factor in EDM since it determines the surface quality of a machined material. An assessment of the SR clearly describes the irregularities found on machined surfaces. Our experimental results showed that amongst the input factors, the pulse current has a significant effect on the surface roughness. There seems to be an upsurge in the discharge energy due to the increase in I_p as it produces a large crater in the surface,[4] which eventually leads to the formation of a rough surface on the workpiece. As shown in **Figure 6a**, the low value of I_p (5–10 A) produces minimum roughness. When I_p (10–15 A) increases, the roughness also increases. This is due to the higher heat generation in the spark zone.[19] When T_{on} is low, the surface roughness is minimum. When T_{on} increases from 40 µs to 120 µs, the surface roughness increases, which is attributed to the longer duration of discharge energy at the spark gap, resulting in higher heat at the workpiece surface.[21] Thus, the surface roughness is found to be better at a lower T_{on} and poorer when it is higher. The influences of the pulse current and gap voltage on the SR are shown in **Figure 6b**. From the graph, it is evident that an increase in the gap voltage causes an increase in the irregularities on the surface. An increase in the voltage leads to a higher energy transfer in the spark zone, producing a coarse surface on the workpiece.[10]

$$SR = -7.42000 + (0.008333\ I_p) + (0.012479\ T_{on}) + (0.34725\ G_V) + (1.5\times10^{-4}\ I_pT_{on}) + (2.5\times10^{-3}\ I_pG_v) + (4.25\times10^{-4}\ T_{on}G_v) + (4.366\times10^{-3}\ I_p^2) - (6.614\times10^{-5}\ T_{on}^2) - (3.20416\times10^{-5}\ G_V^2) \quad (3)$$

The objective of the present investigation is to determine the optimum input factors that provide the maximum MRR and minimum SR. The RSM integrated with GRA technique is utilized to get the desired solution. The grey approach can give a solution for the system where the model is uncertain.[9] The GRA is an adequate method for assessing the relations among the selected responses, with less information on the input factors. This procedure is important for clarifying the complex interrelationships among the response parameters, effectively expressed with the single grey relational grade (GRG). The GRA methodology is an uncomplicated and simple procedure for an optimization calculation.[15] The systematic procedure of implementing the GRA optimization technique is as follows: Firstly, the experimental data is normalized between 0–1 and this is termed as the grey relational generation. Subsequently, all the normalized data is transformed into the grey relational coefficient (GRC) for obtaining the relationship between the desired and actual experimental data. The GRA is evaluated based on its GRG whose values are computed by considering the average of the GRCs of the multi-response fac-

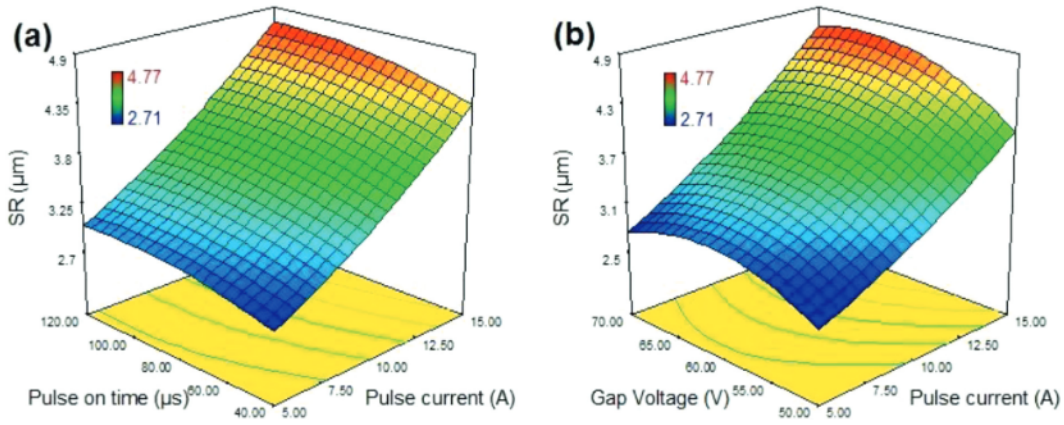

Figure 6: Effects on the SR: a) I_P and T_{on}, b) I_P and G_v

Table 5: Grey relational coefficient and grey relational grade for MRR and SR I_p = 10 A, T_{on} = 40 µs, G_v = 50 V

Sl. No.	Control factors			Responses		Grey relational coefficient (GRC)		Grey relational grade (GRG)	Rank
	I_p/A	T_{on}/µs	G_v/(V)	MRR/(g/min)	SR/µm	MRR/(g/min)	SR/(µm)		
1	10	120	50	0.041	2.97	0.541	0.776	0.658	7
2	10	80	60	0.05	3.77	0.714	0.459	0.587	9
3	***10***	***40***	***50***	***0.045***	***2.97***	***0.606***	***0.776***	***0.691***	***1***
4	5	40	60	0.025	2.71	0.377	1.000	0.689	2
5	15	120	60	0.052	4.77	0.769	0.304	0.537	14
6	15	80	50	0.057	4.03	0.952	0.405	0.679	4
7	10	80	60	0.046	3.58	0.625	0.508	0.567	13
8	5	80	50	0.026	2.73	0.385	0.978	0.681	3
9	15	40	60	0.058	4.42	1.000	0.345	0.672	6
10	10	80	60	0.049	3.77	0.690	0.459	0.574	11
11	15	80	70	0.056	4.51	0.909	0.333	0.621	8
12	5	120	60	0.019	2.94	0.339	0.796	0.568	12
13	10	40	70	0.04	3.25	0.526	0.625	0.576	10
14	5	80	70	0.018	2.71	0.333	1.000	0.667	5
15	10	120	70	0.04	3.93	0.526	0.425	0.475	15

tors for individual experimental runs. In this way, the multi-response objective problem is converted into a single objective problem.

The list of formulae used for calculating the GRG is presented below:

1. Normalization of the selected output responses. Generally, normalization is classified into three types, namely: the higher the better (HB), the lower the better (LB) and the nominal the better (NB). In this study the MRR and SR are selected as the output responses where the MRR follows the HB criteria, while the SR follows the LB criteria and they are expressed with Equations (4) and (5), respectively:

$$y_i(k) = \frac{\max z_i(k) - z_i(k)}{\max z_i(k) - \min z_i(k)} \tag{4}$$

$$y_i(k) = \frac{z_i(k) - \min z_i(k)}{\max z_i(k) - \min z_i(k)} \tag{5}$$

where z_i(k) is the obtained value, min z_i(k) is the minimum value for the k^{th} response and max z_i(k) is the maximum value for the k^{th} response.

2. To determine the deviation for the corresponding process variable, we use Equation (6).

$$\Delta_{oi} = \left| y_0^*(k) - y_i^*(k) \right| \tag{6}$$

where y_0^*(k) is the reference sequence and y_i^*(k) is the comparability sequence. Δ_{0i} is the deviation sequence of the reference sequence and the comparability sequence.

3. For the grey relational coefficient, we use Equation (7):

$$\xi(k) = \frac{\Delta_{min} + \phi\Delta_{max}}{\Delta_{oi}(k) + \phi\Delta_{max}}$$

$$\Delta_{min} = \min_{\forall i} \min_{\forall k} \left\| y_0^*(k) - y_i^*(k) \right\| \tag{7}$$

$$\Delta_{max} = \max_{\forall i} \max_{\forall k} \left\| y_0^*(k) - y_i^*(k) \right\|$$

ϕ is the identification coefficient and its value is 0.5.

4. To calculate the grey relational grade, we use Equation (8):

$$\gamma_i = \frac{1}{n} \sum_{k=1}^{n} \xi_i(k) \tag{8}$$

Based on the normalized value, grey relational coefficients were computed for all the responses, using Equation (7). Finally, the grey relational grade was determined by taking the mean of all the GRCs, using Equation (8). The results of the GRA for the selected responses are shown in **Table 5**. A very important function of the GRG is to convert multiple quality characteristics into a single representative and assign the rank for the GRG from a higher value to a lower value. In **Table 5**, experiment (3) has the highest GRG value, which is 0.691, indicating that the corresponding experiment results are close to the ideal values (I_p = 10 A, T_{on} = 40 µs, G_v = 50 V). The larger the GRG value, the better are the output characteristics; in addition, the specific experimental run exhibits better multiple response characteristics. After the optimal factors influencing the multiple response characteristics were identified, a confirmation test was performed to validate the experimental results. It was computed using the predicted GRG Equation (9). On **Table 6**, it is noted that the predicted and experimental results are in close agreement, indicating that the analysis carried out was successfully implemented. The experimental GRG obtained for the optimal combination of the factors is 0.7215 while its predicted value is 0.6910, which is a nearly 4.41 % improvement in the weight of the GRG. This clearly shows the usefulness of the GRA approach for the optimization of the machining (EDM) parameter where multiple characteristics have to be studied simultaneously.

$$\zeta_{Predict} = \zeta_m + \sum_{i=1}^{f} (\bar{\zeta}_i - \zeta_m) \tag{9}$$

ζ_m is ther total mean grey relational grade, $\bar{\zeta}_i$ is the mean grey grey relational grade at the optimal levels,

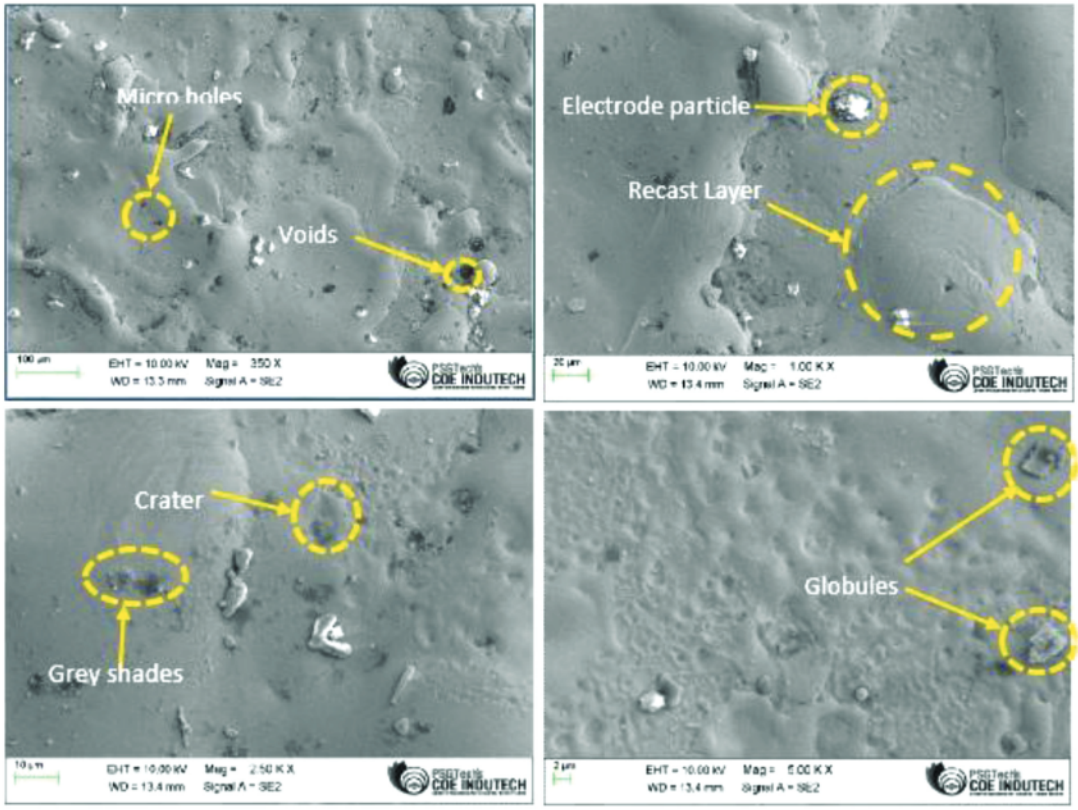

Figure 7: FE-SEM micrographs at optimal parameter settings (I_p = 10 A, T_{on} = 40 µs, G_v = 50 V)

and r is the number factors significantly affecting the overall quality characteristics

Table 6: Result of the confirmation test

GRG value	Predicated value	Experiment	Percentage improvement in the weight of GRG
	0.6910	0.7215	4.41

The surface analysis of the machined part is considered as one of the fundamental tasks in modern applications when producing a costly part. FE-SEM images were captured with a CARL ZEISS machine, USA, with a resolution of 1.5 nm. The surface was examined at various magnifications, namely at 350×, 1000×, 2500× and 5000×. The optimal-run workpiece was selected for the morphological analysis. **Figure 7** shows the SEM surface structures of the Inconel 718 samples. Irregularities in the form of voids, cracks and microholes are noticed on the surfaces. This is mainly due to the high thermal stresses affecting the surfaces during the machining.[18] Recast layers, gray shades and craters are also observed in the images. This is due to the melting of the metal at the high temperature of the discharged sparks between the workpiece and electrode.[20]

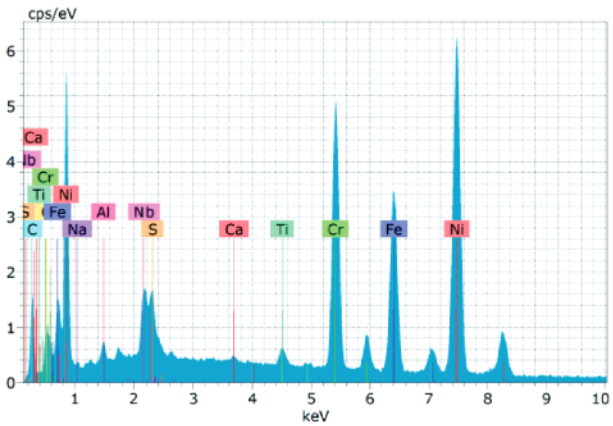

Figure 8: EDAX at optimal level settings (I_p = 10 A, T_{on} = 40 µs, G_v = 50 V)

To further understand the effect of the composite tool on the workpiece surface, an EDAX analysis was done on the machined Inconel 718 surface. **Figure 8** shows the EDAX image obtained for the optimal-run workpiece. The presence of titanium confirms that a certain amount of the tool material was transferred onto the workpiece. The presence of Ni and Cr proves that the selected alloy is Inconel. A high amount of carbon was also observed because of the reactions among dielectric molecules at the elevated temperature. In addition, EDAX also shows some other elements on the surface of the workpiece, viz., Fe, Ca, S, Al, Nb, Na, and O.

4 CONCLUSIONS

A TiB_2-Cu composite PM electrode was developed with powder metallurgy and the behaviour of the tool

electrode was studied during EDM with selected input factors. The key results obtained in this study are reported below:

1. The fabrication of the TiB_2-Cu sintered composite electrode through a powder-metallurgy process is practical and a high MRR (0.057 g/min) was observed at I_p = 15 A, T_{on} = 40 µs and G_v = 60 V.The best surface quality (2.71µm) was observed at a I_p = 5A, T_{on} = 40 µs and G_v = 60 V.
2. Using the ANOVA test, the impacts of the input factors on the MRR and SR were studied. It was found that the pulse current has more influence on the MRR and SR.
3. Optimal parameter settings were identified using the response surface/grey relational analysis. The obtained optimal settings were I_p = 10A, T_{on} = 40 µs and G_v = 50 V.
4. Including a certain amount of titanium, the tool material was transferred to the machined surface at the optimal run. The EDAX analysis indicates that 0.13 % of titanium was transferred onto the machined surface.

5 REFERENCES

[1] S. S. Kumar, T. Varol, A, Canakci, S. T. Kumaran, M. Uthayakumar, A review on the performance of the materials by surface modification through EDM, International Journal of Lightweight Materials and Manufacture, 4 (**2021**) 1, 127–144, doi:10.1016/j.ijlmm.2020.08.002

[2] T. Muthuramalingam, B. Mohan, A review on influence of electrical process parameters in EDM process, Archives of Civil and Mechanical Engineering, 15 (**2015**) 1, 87–94

[3] A. S. Gill, S. Kumar, Investigation of Micro-Hardness in Electrical Discharge Alloying of En31 Tool Steel with Cu–W Powder Metallurgy Electrode, Arabian Journal for Science and Engineering, 43 (**2018**), 1499–1510, doi:10.1007/s13369-017-2960-x

[4] Y. L. Teng, L. Li, W. Zhang, N. Wang, C. C. Feng, H. J. Ren, Machining characteristics of PCD by EDM with Cu-Ni composite electrode, Materials and Manufacturing Processes, 35 (**2020**) 4, 442–448, doi:10.1080/10426914.2020.1718700

[5] A. Sarmah, S. Kar, P. K. Patowari, Surface modification of aluminium with green compact powder metallurgy Inconel-aluminium tool in EDM, Materials and Manufacturing Processes, 35 (**2020**) 10, 1104–1112, doi:10.1080/10426914.2020.1765253

[6] P. M. Kumar, K. Sivakumar, N. Jayakumar, Multiobjective optimization and analysis of copper–titanium diboride electrode in EDM of monel 400™ alloy, Materials and Manufacturing Processes, 33 (**2018**) 13, 1429–1437, doi:10.1080/10426914.2017.1415439

[7] M. Tanjilul, D. N. W. Keong, A. Senthil Kumar, Performance Evaluation of Al2O3 Nano Powder Mixed Dielectric for Electric Discharge Machining of Inconel 825, Materials and Manufacturing Processes, 36 (**2020**) 3, 341–350, doi:10.1080/10426914.2020.1832682

[8] F. Jafarian, Electro discharge machining of Inconel 718 alloy and process optimization, Materials and Manufacturing Processes, 35 (**2020**) 1, 95–103, doi:10.1080 /10426914. 2014.930956

[9] P. Paswan, A. Pramanik, S. Chattopadhyaya, Machining performance of Inconel 718 using graphene nanofluid in EDM, Materials and Manufacturing Processes, 35 (**2020**) 1, 33–42, doi:10.1080/10426914.2020.1711924

[10] S. K. Ramuvel, S. Paramasivam, Study on tool steel machining with ZNC EDM by RSM, GREY and NSGA, Journal of Materials Research and Technology, 9 (**2020**) 3, 3885–3896, doi:10.1016/j.jmrt.2020.02.015

[11] S. Kumar, S. K. Ghoshal, P. K. Arora, L. Nagdeve, Multi-variable optimization in die-sinking EDM process of AISI420 stainless steel, Materials and Manufacturing Processes, 36 (**2020**) 5, 572–582, doi:10.1080/10426914.2020.1843678

[12] R. F. Mazarbhuiya, M. Rahang, Reverse EDM process for pattern generation using powder metallurgical green compact tool, Materials and Manufacturing Processes, 35 (**2020**) 15, 1741–1748, doi:10.1080/10426914.2020.1802036

[13] M. Li, Z. Yang, H. Dong, Y. Zhou, Y. Liu, Machining performance of high energy die-sinking electrical discharge machining on GH2132, Materials and Manufacturing Processes, 35 (**2020**) 9, 1024–1031, doi:10.1080/10426914.2020.1758328

[14] S. Nair, A. Dutta, R. Narayanan, A. Giridharan, Investigation on EDM machining of Ti6Al4V with negative polarity brass electrode, Materials and Manufacturing Processes, 34 (**2019**) 16, 1824–1831, doi:10.1080/10426914.2019.1675891

[15] M. Rahang, P. K. Patowari, Pattern generation by selective area deposition of material in EDM, Materials and Manufacturing Processes, 34 (**2019**) 16, 1847–1854, doi:10.1080/10426914.2019.1669798

[16] A. R. Siddique, S. Mohanty, A. K. Das, Microelectrical discharge coating of Titanium alloy using WS2 and Brass P/M electrode, Materials and Manufacturing Processes, 34 (**2019**) 15, 1761–1774, doi:10.1080/10426914.2019.1666988

[17] P. M. Kumar, K. Sivakumar, N. Jayakumar, Surface Modification on OHNS Steel Using Cu-CrB_2 Green Compact Electrode in EDM, Materials Today: Proceedings, 5 (**2018**) 9, 17389–17395

[18] S. H. Chen, K. T. Huang, Deep hole electrical discharge machining of nickel-based Inconel-718 alloy using response surface methodology, The International Journal of Advanced Manufacturing Technology, 117 (**2021**) 11, 3281–3295, doi:10.1007/s00170-021-07836-3

[19] P. K. Obratanski, K. Zagorski, J. Cieslik, E. Lazaros Papazoglou, A. Markopoulos, Surface Topography of Ti 6Al 4V ELI after High Power EDM, Procedia Manufacturing, 47 (**2020**), 788–794, doi:10.1016/j.promfg.2020.04.242

[20] A. Kumar, A. Mandal, A. R. Dixit, A. K. Das, Performance Evaluation of Al_2O_3 Nano Powder Mixed Dielectric for Electric Discharge Machining of Inconel 825, Materials and Manufacturing Processes, 33 (**2017**) 9, 986–995, doi:10.1080/10426914.2017.1376081

[21] P. Mandal, S. C. Mondal, Surface Characteristics of Mild Steel Using EDM with Cu-MWCNT Composite Electrode, Materials and Manufacturing Processes, 34 (**2019**) 12, 1326–1332, doi:10.1080/10426914.2019.1605179

[22] R. Tyagi, N. K. Mahto, A. K. Das, A. Mandal, Preparation of MoS_2+Cu coating through the EDC process and its analysis, Surface Engineering, 36 (**2020**) 1, 86–93, doi:10.1080/02670844.2019.1615744

[23] R. Sajeevan, A. K. Dubey, Machining quality comparison of Al-TiB_2 composite using conventional EDM and magnetic force-assisted powder-mixed EDM, Advances in Materials and Processing Technologies, (**2021**), doi:10.1080/2374068X.2021.1945299